Deep-Sea Research I 115 (2016) 221–232

Contents lists available at ScienceDirect

Deep-Sea Research I

journal homepage: www.elsevier.com/locate/dsri

Assessing microbial processes in deep-sea hydrothermal systems by incubation at *in situ* temperature and pressure

Jesse McNichol [a], Sean P. Sylva [b], François Thomas [a,1], Craig D. Taylor [a], Stefan M. Sievert [a,*], Jeffrey S. Seewald [b,*]

[a] Biology Department, Woods Hole Oceanographic Institution, Woods Hole, MA 02543, United States
[b] Department of Marine Chemistry and Geochemistry, Woods Hole Oceanographic Institution, Woods Hole, MA 02543, United States

ARTICLE INFO

Article history:
Received 7 March 2016
Received in revised form
2 June 2016
Accepted 15 June 2016
Available online 25 June 2016

Keywords:
Chemolithoautotrophy
Epsilonproteobacteria
Hydrothermal vent
Microbial ecology
Rate measurements
High-pressure incubations

ABSTRACT

At deep-sea hydrothermal vents, a large source of potential chemical energy is created when reducing vent fluid and oxidizing seawater mix. In this environment, chemolithoautotrophic microbes catalyze exergonic redox reactions which in turn provide the energy needed to fuel their growth and the fixation of CO_2 into biomass. In addition to producing new organic matter, this process also consumes compounds contained both in vent fluid and entrained seawater (*e.g.* H_2, NO_3^-). Despite their biogeochemical importance, such reactions have remained difficult to quantify due to methodological limitations. To address this knowledge gap, this study reports a novel application of isobaric gas-tight fluid samplers for conducting incubations of hydrothermal vent fluids at *in situ* temperature and pressure. Eighteen ~24 h incubations were carried out, representing seven distinct conditions that examine amendments consisting of different electron donors and acceptors. Microbial activity was observed in all treatments, and time series chemical measurements showed that activity was limited by electron acceptor supply, confirming predictions based on geochemical data. Also consistent with these predictions, the presence of nitrate increased rates of hydrogen consumption and yielded ammonium as a product of nitrate respiration. The stoichiometry of predicted redox reactions was also determined, revealing that the sulfur and nitrogen cycles are incompletely understood at deep-sea vents, and likely involve unknown intermediate redox species. Finally, the measured rates of redox processes were either equal to or far greater than what has been reported in previous studies where *in situ* conditions were not maintained. In addition to providing insights into deep-sea hydrothermal vent biogeochemistry, the methods described herein also offer a practical approach for the incubation of any deep-sea pelagic sample under *in situ* conditions.

© 2016 Elsevier Ltd. All rights reserved.

1. Introduction

At deep-sea hydrothermal vents, entire ecosystems are supported by primary production in the absence of sunlight. This process, known as chemosynthesis or chemolithoautotrophy, can occur due to chemical disequilibria between reducing hydrothermal vent fluids and oxidizing seawater. Chemosynthetic microbes catalyze thermodynamically-favorable redox reactions and couple this chemical energy to CO_2 fixation, thereby transforming an inorganic energy source into biomass (Jannasch and Mottl, 1985). In addition to supporting productive ecosystems, this process has significant biogeochemical implications. For example, chemosynthetic microbes not only consume reduced inorganic compounds, but they also remove nitrate and oxygen from seawater that mixes with vent fluid.

In the past two decades, the analysis of nucleic acids obtained directly from natural microbial communities as well as the characterization of newly isolated strains of chemolithoautotrophic microbes has revealed insights into the taxonomy, abundance and metabolic potentials of deep-sea vent chemolithoautotrophs (*e.g.* Huber et al., 2007; Nakagawa and Takai, 2008; Sievert and Vetriani, 2012 and references therein). Studies conducted thus far have shown that fluid composition can exert important controls on microbial community structure and function (Amend et al., 2011; Flores et al., 2011, 2012; Dahle et al., 2015; Hentscher and

* Corresponding authors.
E-mail addresses: ssievert@whoi.edu (S.M. Sievert), jseewald@whoi.edu (J.S. Seewald).
[1] Present address: UMR 8227 Integrative Biology of Marine Models, Sorbonne Universités, UPMC Univ Paris 06, CNRS, Station Biologique de Roscoff, CS 90074, Roscoff, France.

http://dx.doi.org/10.1016/j.dsr.2016.06.011
0967-0637/© 2016 Elsevier Ltd. All rights reserved.

Bach, 2012), but the reverse question, *i.e.* how microbes themselves affect fluid composition has received less attention. Although microbial metabolism can be inferred indirectly in low temperature hydrothermal fluids by measuring deviations from the conservative mixing line between high temperature endmember fluids and seawater (Butterfield et al., 2004; Von Damm and Lilley, 2004; Proskurowski et al., 2008; Wankel et al., 2011), this approach cannot provide unequivocal proof that these signatures are microbial nor determine the rates of processes. Therefore, the lack of direct measurements of microbial metabolism hinders our understanding of the biogeochemical role of chemosynthetic processes within vent ecosystems, including their primary productivity (Sievert and Vetriani, 2012).

In order to identify active metabolic pathways and their rates at deep-sea vents, experiments that simulate the natural environment as closely as possible are needed (Sievert and Vetriani, 2012). A conceptually straightforward approach to accomplish this goal is to directly incubate fluids collected from the environment with their resident microbes. This approach is complicated, however, by both inherent challenges of working with deep-sea vent fluids as well as difficulties designing experiments to realistically infer *in situ* processes. Indeed, previous studies have shown that deep-sea microorganisms are sensitive to a decrease in pressure (Bartlett, 2002), suggesting that decompression can affect biological rate measurements. For example, Bianchi et al. (1999) showed that bacterial production rates are underestimated by approximately one half in decompressed pelagic water samples from depths greater than 850 m.

In addition to pressure, the chemical environment is also fundamentally important since the concentration of chemical species directly influences which microbial assimilatory/dissimilatory redox reactions can occur and the rates at which these reactions proceed. The chemical environment in fluid samples collected at deep sea vents may change dramatically if pressure is not maintained during transport to the sea surface due to the loss of volatile species (*i.e.* H_2, H_2S, CH_4, CO_2). This results in the removal of potential energy sources and alteration of key parameters such as pH, which in turn may affect the composition and activity of the indigenous microbial communities. Artifacts may also be introduced during fluid collection from the natural environment if ambient seawater is entrained. The presence of exogenous seawater not only alters the chemical environment, but also introduces a compositionally distinct microbial community not representative of the vent system.

In addition to technical challenges associated with obtaining representative samples of vent fluid, deriving accurate information on *in situ* processes from incubations of this fluid is complicated by the fact that chemolithoautotrophic microorganisms will have already affected the geochemistry of fluids prior to sampling, depleting some chemicals while producing others (Butterfield et al., 2004; Von Damm and Lilley, 2004; Proskurowski et al., 2008; Wankel et al., 2011). The extent of this effect is poorly known, but must be a function of fluid flow rate, absolute concentrations of chemical species, and the abundance of microorganisms and their metabolic rates. Because diffuse-flow hydrothermal environments are characterized by a continuous replenishment of substrate-bearing fluids, microbial communities can be sustained *in situ* even if relevant metabolic redox couples are present at very low concentrations in sampled fluids. Therefore, in closed-system (batch) growth experiments, low concentrations of reactants in energy-yielding redox reactions is problematic since it will be difficult (if not impossible) to measure some processes, despite their likely occurrence in the natural environment.

To circumvent the aforementioned issues, we used an existing hydrothermal fluid sampler to conduct microbial incubations under simulated sea-floor conditions. Isobaric gas-tight (IGT) fluid samplers (Seewald et al., 2002) were designed to maintain fluids at seafloor pressure following collection. They are ideal for sampling low-flow diffuse vents because their slow fill rate ($\sim$75 mL min^{-1}) minimizes the entrainment of ambient seawater and a thermocouple co-located with the sampler inlet snorkel provides real-time temperature information to precisely position the fluid intake in the vent environment. As part of this new application, we developed methods for fluid withdrawals from and additions to the IGT sampler, which allowed both initial chemical amendments and monitoring of substrate concentrations and cell numbers over time, all while maintaining seafloor pressure. Below, we report the results of shipboard experiments designed to improve the understanding of microbial metabolism in deep-sea hydrothermal vent fluids by identifying active chemosynthetic redox reactions, inferring the stoichiometry of these reactions, and quantifying their rates.

2. Materials and methods

2.1. Field site

Vent fluids used for incubation experiments were collected from *Crab Spa* (9°50.3981 N, 104°17.4942 W), a well-studied diffuse-flow hydrothermal vent located on the East Pacific Rise at a depth of 2506 m, using the ROV Jason II deployed from the R/V Atlantis during research cruise AT26-10 in January 2014. At this site, warm fluids ($\sim$24 °C) containing microbes emanate from a well-defined orifice, and have maintained a temporally stable chemical and temperature composition since 2007 (Reeves et al., 2014; Sievert, Seewald, Le Bris and Luther, unpublished data). Prior to the first sampling, the site was allowed to stabilize after megafauna (*e.g.*, *Riftia pachyptila, Bathymodiolus* sp.) were cleared to directly access the fluids emanating from the subseafloor.

2.2. Experimental design and methods for incubations

Similar to other low temperature vent fluids, many chemical species at *Crab Spa* are depleted relative to concentrations expected for mixing of the high temperature endmember source fluid with seawater. Therefore, we chose to conduct replicated amendments of these natural vent fluids with electron acceptors and donors (Table 1). In particular, dissolved nitrate and oxygen were added to test if their presence would stimulate sulfide oxidation, and dissolved hydrogen was added to test whether microbes were capable of hydrogen oxidation, with or without added nitrate. These conditions were compared to controls (no amendments) to confirm that electron donor oxidation was limited by availability of electron acceptors. Since our goal was to mimic the natural environment, most incubations were carried out at 24 °C in the shipboard laboratory, nearly identical to the temperature at which *Crab Spa* fluids exit the seafloor. Two additional incubations were carried out at 50 °C to examine biogeochemical processes at higher temperatures that likely characterize deeper subseafloor environments.

Prior to deployment at the seafloor, the IGT samplers were washed with dilute HCl (pH 3) to remove any residual ^{13}C-labeled dissolved inorganic carbonate (DIC) from previous incubations, followed by a 70% ethanol rinse to sterilize the interior, and acetone to dry the ethanol. A Teflon O-ring was added to the IGT sample chamber prior to deployment to allow fluid stirring following chemical additions and prior to time series sampling during the incubations (Fig. 1). The snorkel and sample valve dead volume ($\sim$4 mL) and sample chamber on the back side of the sample piston were filled with filtered bottom seawater while the accumulator chamber on the backside of the accumulator piston was filled with

Table 1
Summary of conditions during high pressure incubations using IGT fluid samplers.

Amendment[a]	Concentration (μM)	Temperature (°C)	# Replicates	Time from seafloor (h)	Figure
Control	NA	24	3	4, 7, 7	2a
H_2	150	24	3	7, 16, 16	2b
NO_3^-	100	24	3	5, 7, 4	2c
O_2 low	80	24	2	3, 3	2d
O_2 high	110	24	2	5, 5	2d
NO_3^-/H_2	100/150	24	3	7, 3, 4	2e
NO_3^-/H_2	100/150	50	2	4, 3	2f

[a] In addition to $^{13}HCO_3^-$.

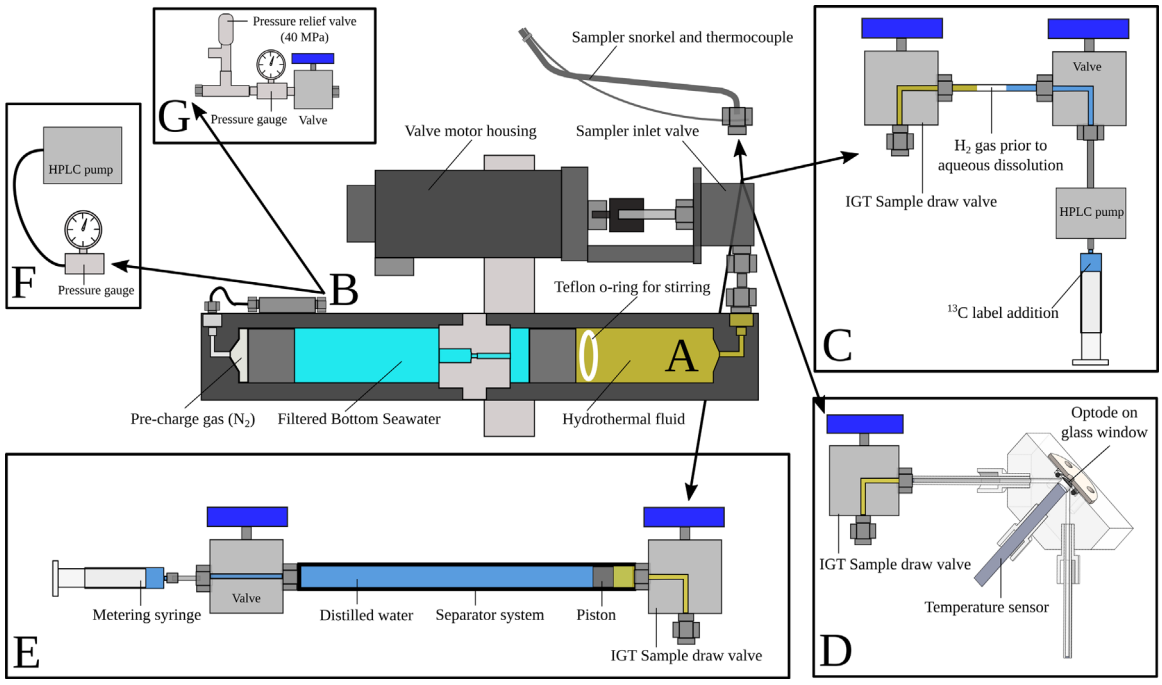

Fig. 1. Isobaric gas-tight (IGT) Sampler configurations used to amend *Crab Spa* hydrothermal fluids with inorganic substrates, monitor chemical consumption, and track microbial growth. For each incubation, the sample draw valve (shown in panel C, D and E) is attached to the sampler inlet valve and is used to regulate fluid flow during both additions of dissolved chemical species and withdrawals for chemical consumption/cell count measurements. Pressure in the IGT is maintained at seafloor values by means of the pre-charge valve (B) which can be opened to bleed off pressure during amendment addition or maintain pressure by adding fluid using an HPLC pump during sample removal (F). In the case of the addition of dissolved hydrogen gas, the configuration in (C) shows how this gaseous substrate was supplied to the sampler. To make instantaneous measurements of dissolved oxygen from IGT fluids, a fiber-optic sensor was held against the optode window in the flow-through cell shown in (D). The separator system (E) used for cell counts allows withdrawals of microbial cells from the sampler without exposure to shear stress. (G) shows the safety setup used for high temperature incubations. The operation of all of these components are explained in greater detail in the text.

compressed nitrogen to ~10% of seafloor pressure at the sampling site (Fig. 1). During sampling, the sampler inlet valve was opened and fluid entering the sampler forced the sample and accumulator pistons to the opposite ends of their respective chambers. Retraction of the accumulator piston compresses nitrogen in the accumulator chamber allowing it to act as a "spring" that buffers internal pressure fluctuations in the sample chamber caused by external temperature changes during transport from the seafloor to the seasurface. Based on 2 °C bottom temperature and 25 °C laboratory temperature, internal pressure increases due to sampler warming are < 15%.

Vent fluid sampling was performed by positioning the IGT snorkel/thermocouple into the orifice of *Crab Spa* until temperature readings reached a stable maximum of at least 23–24 °C, at which point the sampler inlet valve was opened. The sampler was allowed to fill for 2 min, and then the sampler inlet valve was closed to retain pressure during transit back to the surface. After retrieval of the IGT samplers on board the ship, a limited number of fluid aliquots (~10 mL total volume) were removed for analysis of selected chemical species. Dissolved methane was used as a conservative tracer for the amount of endmember hydrothermal fluid in a given sample. Fluids were not used for incubations if the methane concentration was < 4 μM, an indication that substantial inadvertent seawater entrainment had occurred during fluid collection. Most shipboard incubations were started within seven hours from sampling at the seafloor, although two IGT samplers used for hydrogen-amended incubations were stored at room temperature for approximately sixteen hours prior to the beginning of the experiment (Table 1).

To compensate for pressure loss during fluid withdrawals from the sample chamber, a high performance liquid chromatography (HPLC) pump (Fig. 1F) was connected to the pre-charge valve (an on/off high-pressure needle valve; Fig. 1B). Distilled water was then pumped into the accumulator chamber until the desired pressure was reached. For fluid additions to the sample chamber, the HPLC pump was connected to the sampler inlet valve to pump in amendments. To relieve excess pressure caused by fluid additions, the pre-charge valve (Fig. 1B) was opened briefly as necessary. In both cases, pressure was monitored using a high-pressure gauge connected to the HPLC pump.

Incubations were initiated by sequentially injecting solutions of known composition. For all additions, the total volume of fluid injected was ~10 mL, which represents 6–7% of the total volume of the IGT sampler (150 mL). The first fluid to be injected was 2 mL of a $NaH^{13}CO_3$ (99% ^{13}C, Cambridge Isotope laboratories) solution of known concentration made up in N_2-purged filtered bottom seawater. This was immediately followed by 8 mL of filtered bottom seawater containing chemical species for each of the incubations indicated in Table 1, at a concentration that would yield the desired abundances after mixing with the vent fluid already in the IGT sample chamber. For all treatments, the final concentration of ^{13}C after injection was ~10% of the total DIC (Supplemental spreadsheet). Immediately after injection, the IGT samplers were rotated 180° several times to allow the Teflon O-ring to fall through the sample chamber, thereby mixing the fluid contents. Following addition of substrates, fluid chemistry and cell abundance were monitored over an 18–24 h period by extracting fluid aliquots from the IGT sample chamber after selected time intervals.

Stock solutions for injection of nitrate, oxygen, and hydrogen were prepared just prior to addition to the IGT sampler. The ^{13}C-bicarbonate solution was used within three days of preparation and refrigerated when not in use. Solutions were prepared anoxically in Hungate tubes or Pyrex bottles, and all glassware was muffled at 480 °C for 4 h prior to use to remove organic contaminants.

Dissolved oxygen was added as a solution of filtered bottom seawater saturated with ultra-high purity O_2 at atmospheric partial pressure (0.103 MPa) for the lower oxygen concentration incubations and in a solution saturated at 0.206 MPa O_2 partial pressure for the higher concentration incubations. Nitrate solutions were prepared from reagent grade $NaNO_3$ dissolved in N_2-purged filtered bottom seawater.

Due to the low solubility of hydrogen gas in aqueous solution, a modified approach involving the HPLC pump was used to amend the incubations with dissolved hydrogen (Fig. 1C). A length of 1/8″ stainless steel tubing with an internal volume of 2 mL was prefilled with hydrogen gas at atmospheric pressure and connected to the IGT sample inlet valve at one end and the HPLC pump outlet at the other. One mL of the filtered bottom seawater/^{13}C label solution was then pumped into the length of hydrogen-filled stainless steel tubing before opening the IGT sample valve, which allowed vent fluid into the sample loop, raising the a pressure to 25 MPa. This solution was allowed to equilibrate for 30 min so that the compressed hydrogen gas could dissolve into the filtered bottom seawater/vent fluid mixture. Once dissolved, the contents of the 1/8″ stainless tube were injected into the sample chamber using the HPLC pump.

Incubations were conducted in the IGT samplers either at *in situ* vent temperature (~24 °C) in the ship's laboratory or at 50 °C by placing them in an oven. Safety considerations necessitated the addition of a 40 MPa pressure-relief connected to the precharge valve to relieve pressure in the event of runaway temperature within the oven (Fig. 1G). Temperature inside the oven was continuously logged at 5 min intervals for all treatments with iButton temperature recorders (Maxim Integrated, San Jose, CA).

In addition to the unamended controls described above, killed controls were conducted to examine abiotic processes. Abiotic sulfide oxidation with oxygen was tested at 24 °C and 50 °C in duplicate experiments by injecting formaldehyde into the IGT sampler to attain a final concentration of 2%, followed by the addition of dissolved oxygen (> 80 μM) and monitoring the sulfide concentration over time. To test if H_2 diffusion or leakage from the IGT sampler was occurring, H_2 was added to a sampler filled with oxic deionized water and the concentration monitored over time at 24 °C. Both controls were conducted on the same timescale as the actual experiments (~24 h).

2.3. Analytical methods

Fluid Chemistry: Total dissolved sulfide ($\Sigma H_2S = H_2S + HS^- + S^{2-}$) was determined potentiometrically using a sulfide-selective electrode. The electrode was calibrated daily with a serial dilution of a standard sodium sulfide solution. pH (25 °C) was measured in fluids withdrawn from the IGT sampler with a Ag/AgCl combination reference electrode calibrated daily. Dissolved methane and hydrogen concentrations were determined shipboard using a gas chromatograph equipped with a 5 Å molecular sieve packed column and serially connected thermal conductivity and flame ionization detectors following quantitative headspace extraction. DIC concentrations ($DIC = CO_3^{2-} + HCO_3^- + H_2CO_3^*$) were determined after fluid acidification with 25 wt% phosphoric acid by injecting aliquots of headspace gas directly into a gas chromatograph equipped with a Porapak-Q packed column and a thermal conductivity detector. Dissolved Mg, Cl and SO_4^{2-} concentrations were analysed by ion chromatography with suppressed conductivity detection. Dissolved oxygen concentrations in IGT samplers were determined by passing hydrothermal fluid through a custom designed flow-through cell fitted with a commercially available oxygen optode and associated temperature probe (Pts3, Presens, Germany; see Fig. 1D). The oxygen optode spot was calibrated with oxygen-free water (treated with sodium dithionite) and air-saturated water. Prior to measurements, the optode flow-through cell was flushed with N_2-purged filtered bottom seawater or deionized water to remove air bubbles. Oxygen levels were determined *in situ* by placing an oxygen optode system directly into hydrothermal fluid flow (Model 4330F; Aanderaa Data Instruments, Fall River, MA), which was calibrated by the manufacturer prior to deployment.

For determination of dissolved nitrate and ammonium concentrations, fluids were filtered shipboard through a 0.2 μm GTTP membrane (Millipore) and stored frozen at −20 °C. The concentration of total nitrate+nitrite was determined on shore by conversion to NO and chemiluminescent detection using a NoxBox instrument (Teledyne, San Diego CA, USA) following the original protocol (Garside, 1982). The concentration of total dissolved ammonia ($\Sigma NH_3 = NH_4^+ + NH_3$) was determined on filtered samples on board the ship by flow injection analysis as previously described (Hall and Aller, 1992).

Fluid aliquots for total cells counts were removed from the IGT samplers using a separator piston system (Fig. 1E), which permitted withdrawal of fluid from the sample chamber with the sample inlet valve completely open. This strategy prevented the shearing and rupture of cells, which would otherwise have occurred by throttling the sample through the small opening in the sample valve stem that would have been required to maintain a high pressure drop across the valve. Fluids are removed by throttling deionized water on the backside of the separator piston into a metering syringe through an additional high pressure valve attached to the separator tube. Pressure inside the IGT sampler moves the separator piston allowing it to fill with fluid from an incubation, which is then recovered by closing the IGT sample inlet valve, disconnecting the separator and forcing the hydrothermal fluid out with the metering syringe.

Cells were preserved by mixing 1.5 mL of fluid with 40 μL of borate-buffered formalin, stained with 200 μL of 0.1% acridine orange solution (Fisher Scientific), filtered under gentle vacuum onto black 0.2 μm polycarbonate filters (GE Healthcare), and enumerated shipboard by fluorescence microscopy (Axioskop 40, Zeiss, Germany). Ten grids were counted per sample and the result extrapolated to the total filtration area to determine the cell concentration. All counts were done in analytical duplicates.

Catalyzed reporter deposition fluorescence in situ hybridization

(CARD-FISH): Aliquots of approximately 10 mL of culture were preserved at ~16 and ~24 h after the addition of labels/amendments with paraformaldehyde (1%) and kept for 1 h at room temperature to fix cells. Cells were then filtered under moderate vacuum onto Au/Pd-sputtered 0.2 μm polycarbonate filters (Millipore), washed 2 × with 10 mL 1 × PBS, air-dried and stored at −20 °C prior to further analysis. Filters were subsequently sectioned, embedded in low-melting point agarose, and endogenous peroxidases were inactivated by immersion in 3% H_2O_2 for 10 min. Horseradish-peroxidase labeled probes (Biomers) were hybridized at 46 °C for 3 h. Tyramide amplification with Oregon Green 488-X (Molecular Probes, Inc.) was conducted for 20 min at 46 °C. Both oligonucleotide probe combinations EPSI549/EPSI914 (Lin et al., 2006; Greuter et al., 2016) and EUBI-III (Daims et al., 1999) were hybridized at 35% formamide.

3. Results

3.1. Crab Spa Microbial community composition and fluid chemistry

All of the *Crab Spa* fluid samples used for this study had similar chemical concentrations that were consistently different from background seawater (Table 2). CARD-FISH counts demonstrated that the microbial communities in the natural fluids were dominated by *Epsilonproteobacteria* (~80% of total cells, Table 3). Fluids contained elevated levels of methane (~6 μM), sulfide (~190 μM) and ammonium (~11.5 μM), and were slightly acidic (pH=5.6), as well as being depleted in oxygen and nitrate relative to seawater (~22 and 6.8 μM, respectively). Oxygen concentrations measured *in situ* were lower than those measured in the IGT samplers (3.6 μM *vs* ≥15 μM). This excess oxygen can be attributed to air-saturated seawater which was used to fill the sampler dead volume. Small air bubbles entrained in the snorkel tips during vehicle deployment may account for occasional high values observed without oxygen amendments (up to 45 μM O_2).

The formation of low temperature vent fluids at oceanic spreading centers occurs as a result of the mixing of high temperature seawater-derived hydrothermal fluids with cold seawater in subseafloor environments (Butterfield et al., 2004; Von Damm and Lilley, 2004). At *Crab Spa*, a likely candidate for the high temperature endmember is the *Tica* vent (located ~14 m NE of *Crab Spa*) which was venting at 194 °C during the course of this study. Based on a two-component mixing model for the formation of the *Crab Spa* fluids involving the endmember *Tica* vent fluid and seawater, concentrations of dissolved sulfide, hydrogen, nitrate and oxygen are substantially depleted indicating consumption following mixing in subsurface environments (Table 2).

Table 3
Percentage of DAPI-stained cells hybridizing to specific CARD-FISH probes in *Crab Spa* vent fluids and experimental amendments of *Crab Spa* fluids after 16–24 h of incubation.

Treatment	EUBI-III-hybridized cells (% DAPI)	EPSI549/914-hybridized cells (% DAPI)
Crab Spa fluid, no incubation (n=2)	93.6 ± 1.0	80.3 ± 4.2
Control, 24 °C (n=3)	94.0 ± 4.2	87.9 ± 18.4
H_2 amend., 24 °C (n=3)	94.2 ± 6.4	81.8 ± 14.8
NO_3^- amend., 24 °C (n=3)	100.7 ± 1.4	97.8 ± 2.7
O_2 amend. 80 μM,24 °C (n=2)	96.5 ± 0.3	100.1 ± 2.8
O_2 amend. 110 μM, 24 °C (n=2)	96.2 ± 1.9	99.2 ± 0.1
NO_3^-/H_2 amend., 24 °C (n=3)	99.0 ± 0.5	100.2 ± 4.3
NO_3^-/H_2 amend., 50 °C (n=2)	95.8 ± 1.4	97.2 ± 3.6

Values shown are averages from 2 to 3 biological replicates with the standard deviation (n=3) or range (n=2) as error.

3.2. Incubation results

In all cases, the natural microbial community remained dominated by *Epsilonproteobacteria*, and in some cases, showed an enrichment compared to background samples (Table 3). Below, we detail specific observations for each condition.

Control treatment (Fig. 2a): In this case, the only addition to fluids was a ^{13}C bicarbonate label. Although cell numbers did not change consistently during incubation, a clear and replicable pattern in chemical concentrations was observed. Sulfide dropped by ~100 μM in all replicates and stabilized at 90–100 μM for the remainder of the experiment, while low initial levels of nitrate and oxygen decreased below the detection limits of ~1 and ~5 μM, respectively. Ammonium concentrations decreased initially by 5–10 μM in two of the replicates, which were elevated at the beginning of the incubation for unknown reasons.

Hydrogen additions (Fig. 2b): The hydrogen-amended incubations were characterized by a pattern of chemical depletion that was similar to the control treatment. In this case, sulfide concentrations decreased by ~100 μM initially, and neither hydrogen nor sulfide were exhausted during the incubation period. Hydrogen decreased slowly in all three replicates, with a concomitant increase in sulfide for the last three time points. Cell concentrations either did not show a consistent trend or increased gradually. Ammonium increased slightly in two replicates and decreased slightly in one, and nitrate and oxygen were exhausted rapidly as in the control treatment to concentrations below their detection limits. Initial sulfide concentrations were lower for the two IGT sampler incubations that were started after a ~10 h delay.

Table 2
Measured and predicted concentrations[a] of selected aqueous species at the *Crab Spa* vent. The endmember concentrations for seawater and the high temperature Tica vent were used to predict the *Crab Spa* abundances.

	pH 25 °C	Mg mm	H_2 μM	H_2S μM	SO_4^{2-} mm	O_2 μm	NO_3^- μM	NH_4^+ μm	CH_4 μM	DIC mm	Cl mm
Tica Endmember	4.3[b]	0[c]	410	7710	<0.5	0[c]	0[c]	2.6[d]	113	85	358
Crab Spa Vent Fluid[e]	5.6	49.2	<2	184	26.5	3.6[f]	6.3	11.9	6.3	8.2	546
Crab Spa Predicted	–	49.2	29	552	25.8	107	32	0.2	8.1	8.2	526
Bottom Seawater	7.9	53.0	<2	<1	27.7	115	34	0	<0.002	2.3	539

[a] mm=mmol/kg fluid, μm=μmol/kg fluid, mM = mmol/L fluid, μM=μmol/L fluid.
[b] Not extrapolated to zero-Mg. Measured in sample containing 12.4 mm Mg.
[c] Assumed endmember value for high-temperature Tica vent fluids.
[d] Data from Reeves et al. (2014).
[e] Corrected for sampler dead volume except for pH.
[f] Measured in situ with oxygen optode system.

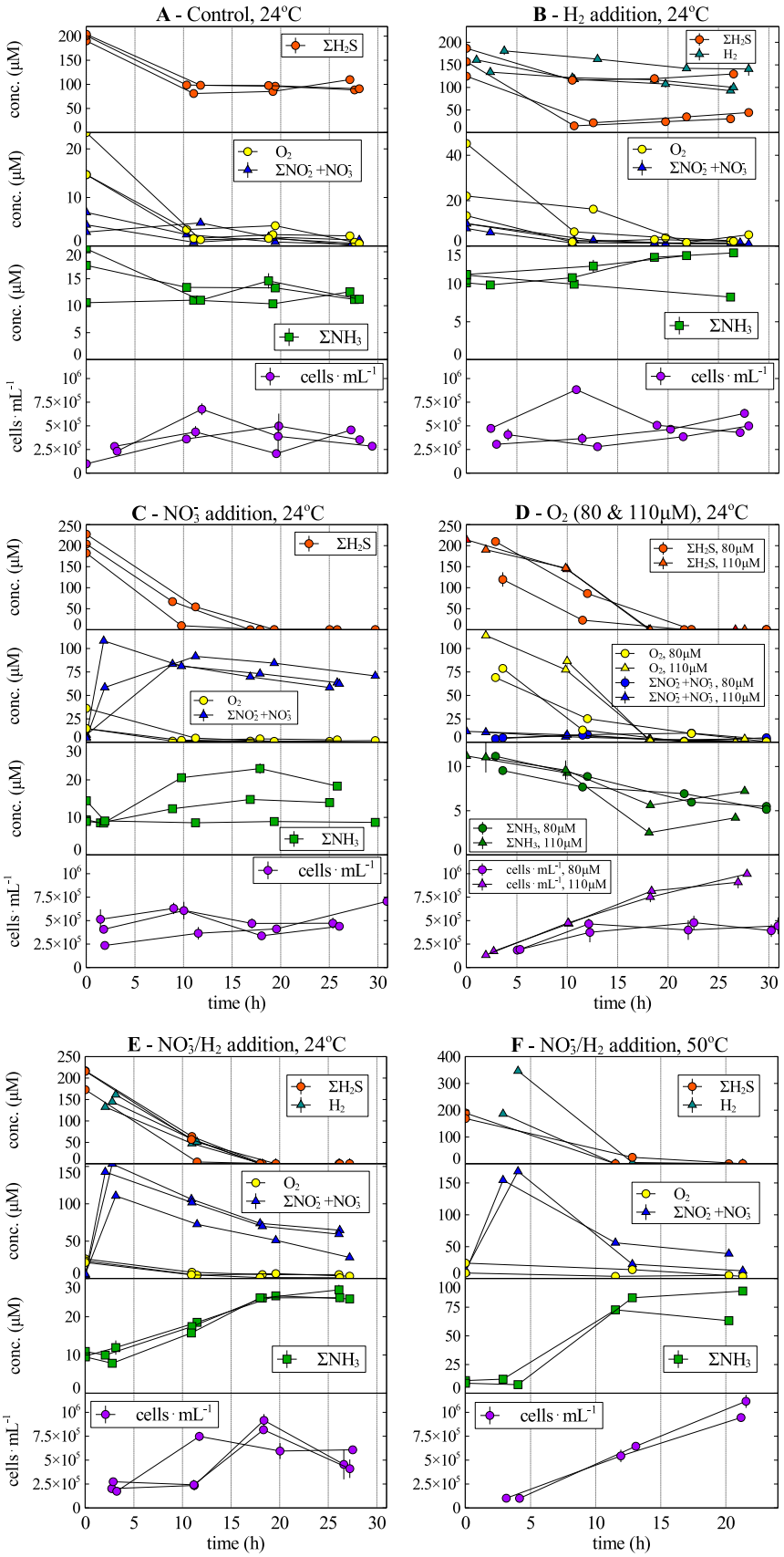

Fig. 2. Incubation results for 6 different treatment types. With the exception of (f), all incubations were carried out at 24 °C. (a) Control, only $^{13}CO_2$ label in anaerobic filtered bottom seawater, (b) Hydrogen additions, (c) Nitrate additions, (d) Oxygen additions, (e) Nitrate/hydrogen additions, (f) Nitrate/hydrogen additions (50 °C). For the oxygen additions, triangles indicate the higher oxygen treatment (110 µM) and circles denote the lower oxygen treatment (80 µM).

Nitrate additions (Fig. 2c): Upon the addition of nitrate, sulfide concentrations decreased to below detection after ~12–18 h. Oxygen was fully depleted after the second time point, and nitrate concentrations gradually decreased throughout the incubations. Ammonium increased in two out of three replicates and cell concentrations either increased gradually during incubations or showed no consistent pattern.

Oxygen additions (Fig. 2d): For the oxygen amended incubations conducted at both 80 and 110 μM, sulfide and oxygen reached levels below detection after 12–18 h. Cell counts were consistent between replicates with an initial increase at ~80 μM after 7 h and a continuous increase at ~110 μM throughout the duration of the incubation. Nitrate was eventually depleted across all treatments, although a transient increase was observed in both ~80 μM oxygen replicates. Ammonium decreased in all incubations by ~5 μM.

Nitrate/hydrogen additions at 24 °C (Fig. 2e): These incubations were characterized by a complete exhaustion of hydrogen, sulfide, and oxygen and a gradual decrease in nitrate. A consistent and replicable increase in ammonium of around 20 μM was observed for all replicates, and cell concentrations increased from the first time point for all incubations, though later decreased in two cases.

Nitrate/hydrogen additions at 50 °C (Fig. 2f): In these treatments, a continuous increase in cell numbers was observed, accompanied by complete exhaustion of oxygen, hydrogen, sulfide and a large decrease in nitrate. A large increase in ammonium of ~60 μM was observed for both replicates.

Killed controls at 24 and 50 °C (Supplemental spreadsheet): For two killed controls at 24 °C, sulfide decreased between 6–20 μM over a 17 h period, whereas at 50 °C, sulfide either decreased by ~30 μM or increased slightly (18 μM) over a 12 h period. Although oxygen concentrations did decrease in some controls, levels never dropped below 94 μM.

4. Discussion

Our study quantified concentrations of redox reactive species and cellular abundance during short-term laboratory incubations of deep-sea hydrothermal vent fluid, allowing biogeochemical processes to be carefully tracked (Fig. 2). Since these incubations were carried out at deep-sea pressure and temperature with μM concentrations of amendments (Table 1), conditions were only slightly altered from the natural environment. Preservation of natural microbial community structure during the incubations (Table 3) suggests that our data may accurately reflect processes occurring in the natural environment. Below, we discuss how the incubations results can be used to confirm hypotheses derived from observations of *in situ* chemistry, infer the stoichiometry of microbially-mediated processes by quantifying redox reactions catalyzed by the community, and determine the rates of microbial processes (Table 5).

4.1. Chemosynthesis at Crab Spa

Models for the formation of low temperature ridge-crest hydrothermal fluids involve two-component mixing of a high temperature Mg-free endmember hydrothermal fluid with Mg-rich (53 mM Mg) seawater. Within the context of such a model, the Mg content of low temperature fluids provides a direct constraint on the relative contributions of the high-temperature endmember and seawater. The Mg content of the *Crab Spa* fluid (49.3 mM) indicates mixing between seawater and hydrothermal end-member fluid at a ratio of approximately 14:1 (Table 2). This mixing ratio has remained relatively constant over time at *Crab Spa*, since it has been observed that fluids have maintained similar temperature, chemistry and microbial composition since 2007 (Reeves et al., 2014; Sievert, Seewald, Le Bris and Luther, unpublished data). The fluids also carry a strong imprint of subseafloor microbial activity as evidenced by depletions of redox sensitive chemical species such as oxygen, nitrate, sulfide, and hydrogen relative to values predicted for conservative mixing, and enrichment of other species such as ammonium (Table 2). Supporting this presumed microbial activity, both freshly sampled and incubated fluids were dominated by *Epsilonproteobacteria* (Table 3), which are well-known to utilize or produce these compounds during their metabolism (Sievert and Vetriani, 2012; Nakagawa and Takai, 2008).

Although sulfate and carbon dioxide are quantitatively the most abundant electron acceptors in these fluids, nitrate, oxygen and intermediate sulfur species (*i.e.* elemental sulfur, polysulfides) are the only electron acceptors present that are known to be utilized by autotrophic *Epsilonproteobacteria* to generate energy in combination with sulfide or hydrogen as electron donors (Sievert and Vetriani, 2012, Fig. 2). Redox reactions involving these chemical species likely support autotrophic microbes *in situ*, but evidence is currently lacking for which are preferentially utilized by microbes and which chemicals ultimately limit energy-generating chemosynthetic reactions. Important clues about these questions can be found in the chemistry of *Crab Spa* fluids, where both oxygen and nitrate are depleted relative to predictions based on conservative mixing, while sulfide remains high (~190 μM). This depletion of electron acceptors is most apparent for oxygen, where *in situ* measurements yielded a value of 3.6 μM, ~103 μM less than predicted for conservative mixing (Table 2).

While oxygen and nitrate concentrations measured *in situ* are very low, they would still be more than sufficient to support chemosynthesis in the natural environment if they were available to microbes at these levels. However, since oxygen was measured in exiting fluids just outside the vent orifice, turbulent mixing with ambient seawater could have introduced oxygen not present in the subseafloor. In addition, even if 3.6 μM is an accurate value for subseafloor fluids, it is likely that there are microenvironments in which these reactants are further depleted, such as in biofilms in the subsurface biosphere. In such an environment, high densities of microbes would likely draw nitrate and oxygen down to much lower levels and ultimately the diffusion of these electron acceptors would limit energy-generating chemosynthetic reactions despite electron donors being present at high concentrations.

Our results support this conjecture by clearly showing that sulfide cannot be completely consumed during experiments (Figs. 2a, b) without the addition of either nitrate or oxygen (Fig. 2c-f). The observed depletions in dissolved sulfide are unlikely to be the result of abiotic oxidation with O_2 since killed controls showed no or very low levels of sulfide and oxygen consumption (see Supplementary spreadsheet), consistent with other studies assessing the role of biotic and abiotic processes in sulfide oxidation (Luther et al., 2011). In addition, robust growth of *Epsilonproteobacteria* was associated with sulfide consumption in the presence of oxygen (Fig. 2d, Table 3), strongly suggesting that microbial sulfide oxidation is tied to oxygen in these incubations (see Table 4 for likely metabolic reactions). In contrast to the oxygen addition experiments, nitrate additions did not result in a consistent pattern of growth, despite rapid and complete consumption of sulfide and enrichment of *Epsilonproteobacteria* compared to background samples (Table 3). This observation, combined with the fact that nitrate was consumed more slowly than oxygen (Table 5), suggests that oxygen serves as the preferred electron acceptor *in situ*, in line with higher growth yields predicted for oxygen relative to nitrate (Chen and Strous, 2013), a phenomenon that has been observed previously in chemostat cultures of *Epsilonproteobacteria* (Timmer-Ten Hoor, 1981).

Table 4
Important predicted redox reactions in incubations of *Crab Spa* fluids that are most likely microbially catalyzed. These reactions are used in subsequent calculations of redox stoichiometry (see Sections 2 and 4).

Equation #	Predicted microbially catalyzed reaction	Description	Evidence for reaction
1	$2H_2S+O_2=>2S^0+2H_2O$	Sulfide oxidation to sulfur coupled to oxygen reduction	O_2 additions
2	$2.5H_2S+H^++NO_3^-=>2.5S^0+3H_2O+0.5N_2$	Sulfide oxidation to sulfur coupled to denitrification	NO_3^- additions
3	$4H_2S+4H^++NO_3^-=>4S^0+3H_2O+2H^++NH_4^+$	Sulfide oxidation to sulfur coupled to DNRA[a]	H_2 and NO_3^- additions
4	$2H_2+O_2=>2H_2O$	Hydrogen oxidation coupled to oxygen reduction	H_2 and H_2/NO_3^- additions
5	$2.5H_2+H^++NO_3^-=>3H_2O+0.5N_2$	Hydrogen oxidation coupled to denitrification	H_2 and H_2/NO_3^- additions
6	$4H_2+2H^++NO_3^-=>3H_2O+NH_4^+$	Hydrogen oxidation coupled to DNRA[a]	H_2 and H_2/NO_3^- additions
7	$H_2+S^0=>H_2S$	Hydrogen oxidation coupled to sulfur reduction	H_2 additions

[a] DNRA=Dissimilatory nitrate reduction to ammonium.

Table 5
Summary of rates of change in chemical concentrations and cell densities.

	Incubation condition						
	Control (24 °C)	**H_2 addition (24 °C)**	**NO_3^- addition (24 °C)**	**O_2 (80 μM) (24 °C)**	**O_2 (110 μM) (24 °C)**	**NO_3^-/H_2 (24 °C)**	**NO_3^-/H_2 (50 °C)**
H_2S consumption (fmol cell^{-1} d^{-1})	475.8	434.3	598.4			527.1	
	797.1	681.6	506.7	483.2	494.5	510.6	312.5
	642.7	238.6	481.7	776.5	523.3	458.1	753.9
H_2S production (fmol cell^{-1} d^{-1})		77.8					
	N.A.	51.7	N.A.	N.A.	N.A.	N.A.	N.A.
		30.6					
H_2 consumption (fmol cell^{-1} d^{-1})		87.9				418.1	
	N.A.	138.5	N.A.	N.A.	N.A.	351.8	1535.2
		49.6				508.4	989.7
O_2 consumption (fmol cell^{-1} d^{-1})	N.R.	N.R.	N.R.	604.4	290.4	N.R.	N.R.
				347.2	608.5		
NO_3^- consumption (fmol cell^{-1} d^{-1})			57.5			229.9	
	N.R.	N.R.	65.0	N.R.	N.R.	193.0	654.7
			87.9			187.7	522.2
NH_4^+ production (fmol cell^{-1} d^{-1})	−42.9	6.1	0			37.8	
	−31.8	−5.7	13.5	−12.2	−14.1	33.0	229.5
	4.9	6.4	37.3	−15.2	−21.3	41.9	245.7
% NO_3^- to DNRA at t_{end}	0	27.9	0			17.5	
	0	0	11.8	0	0	19.4	55.2
	48.5	63.2	21.1	0	0	18.2	53.1
Initial cell density (× 10^5 cells mL^{-1})	2.3	4.1	2.4			2.7	
	9.8	3.1	5.1	1.9	1.3	2.0	1.0
	2.8	4.7	4.1	1.9	1.7	1.7	1.0
Maximum cell density (× 10^5 cells mL^{-1})	6.8	5.0	7.1			8.2	
	5.0	6.3	6.3	4.7	10.0	9.2	11.2
	4.6	8.8	6.1	4.8	9.1	7.5	9.5

N.A.=Not applicable, process not observed. N.R.=Data not reported. In these cases data is not presented because the resolution of time series measurements is too low to capture accurate rates. This is due to the low initial concentrations of the analyte in question. Cell-specific rates during incubations were calculated by dividing volumetric rates by the average of initial and maximum cell densities.

In addition to sulfide, hydrogen oxidation also has the potential to be an important process supporting chemolithoautotrophic production at vents, since it can support higher growth rates and/or yields than sulfide oxidation in autotrophic *Epsilonproteobacteria* (Takai et al., 2006; Han and Perner, 2014). Although present in endmember fluids, hydrogen is barely detectable upon sampling at *Crab Spa* (Table 2), suggesting that microbes in the subseafloor are actively consuming it by coupling its oxidation to either oxygen, nitrate or sulfur reduction. Supporting this idea, hydrogen was rapidly and completely consumed in incubations that also received nitrate (Fig. 2e, f), and consumed more slowly in incubations to which only hydrogen was added (Fig. 2b). As with sulfide, this oxidation was almost certainly microbially-mediated since abiotic H_2 oxidation by oxygen is kinetically inhibited at the incubation temperatures (Foustoukos et al., 2011). It is noteworthy that drawdown of hydrogen continued after the depletion of nitrate/oxygen and was accompanied by a steady increase in the concentration of sulfide (Fig. 2b). This increase in sulfide was most

likely due to the oxidation of hydrogen coupled to the respiration of oxidized sulfur species. Although dissimilatory sulfate reduction could potentially result in such sulfide production, it is unlikely to have occurred in these incubations since this process has not been reported in *Epsilonproteobacteria*, which dominated the incubations (Table 3). In contrast, there is ample evidence that *Epsilonproteobacteria* can catalyze the oxidation of hydrogen coupled to the respiration of intermediate sulfur species such as polysulfide, elemental sulfur or thiosulfate (Hedderich et al., 1998; Sievert and Vetriani, 2012 and references therein; Mino et al., 2014). However, it should be noted that sulfur species with intermediate oxidation states are likely quantitatively less important than oxygen or nitrate as electron acceptors *in situ*, since sulfide production was only observed at hydrogen concentrations 3–4 times the maximum predicted for the natural environment (Table 2), and only after oxygen and nitrate were both depleted.

Together, these results provide direct evidence that depletions of redox-active chemicals at *Crab Spa* are microbially mediated, and that the supply of electron acceptors limits chemosynthesis *in situ*. Although methane is present at ~6 μM in *Crab Spa* fluids, it was not consumed during incubation experiments even at high oxygen tensions (data not shown). The lack of methane oxidation could be due to the competitive exclusion of methanotrophic communities *in situ* by fast-respiring *Epsilonproteobacteria* drawing oxygen and nitrate down to levels below which aerobic or denitrifying methanotrophs could survive. In this case, the sampled fluids in our study would not contain large populations of methanotrophs. This appears to be the case at the Menez Gwen hydrothermal vent field, where metagenomes indicate the absence of known methane-oxidizing genes (Meier et al., 2016), despite the end-member fluids being rich in methane (Charlou et al., 2000).

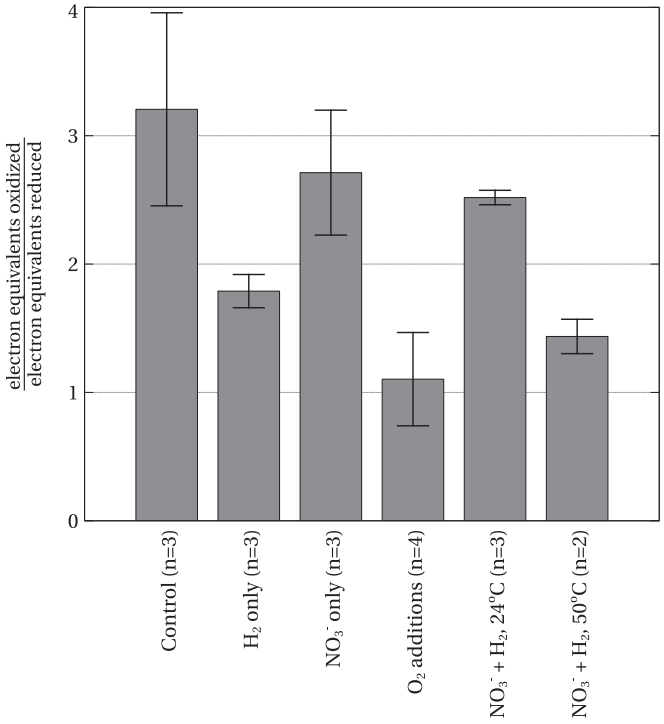

Fig. 3. Community redox balance for IGT incubations represented as a ratio. A ratio of one indicates balanced use of electron donors and acceptors and a ratio greater than one indicates that more electron donor was consumed than could be accounted for by consumption of electron acceptors (according to the assumptions outlined in the text). Errors are either standard deviations (n > 2), or ranges (n = 2).

4.2. Biogeochemistry of sulfur and nitrogen

While the above discussion paints a general picture of processes underlying chemosynthesis at. *Crab Spa*, incubation results can also be used to determine the stoichiometry of oxidation and reduction reactions catalyzed by microbes, which in turn constrains possible biochemical mechanisms. For example, in all incubations, the amount of nitrate and oxygen consumed was never sufficient to account for the complete oxidation of sulfide to sulfate (Supplemental spreadsheet), suggesting that sulfide was oxidized to an intermediate oxidation state sulfur species. Some autotrophic *Epsilonproteobacteria* can catalyze sulfide oxidation to elemental sulfur (S^0) (Wirsen et al., 2002; Sievert et al., 2007), and indeed white flocculent material (likely composed of S^0) continuously emanates from *Crab Spa*.

In order to test whether this was occurring in our incubations, the overall redox balance between the total amounts of electron donors and acceptors consumed was determined. This was accomplished by using the reactions summarized in Table 4 to calculate the ratio of electrons transferred from electron donor to acceptor as indicated by changes in the concentrations of relevant chemical species. A ratio of one indicates a balance between the consumption of electron donors and acceptors, and examination of Fig. 3 reveals that the only treatment where electron donors and acceptors were balanced was for the oxygen additions. In contrast, values greater than one were observed for all of the other conditions, indicating that the amount of electrons predicted to be transferred due to oxidation of electron donors exceeds the amount that can be accounted for by the changes in the concentrations of electron acceptors - even assuming that sulfide was oxidized to the intermediate S^0. Although alternative electron acceptors used in microbial respiration could potentially account for this imbalance, we know of no other candidate electron acceptors at *Crab Spa* that could support additional sulfide oxidation.

However, an alternative possibility which can consume sulfide without requiring additional microbial respiration is the abiotic production of polysulfide by reaction of sulfide with elemental sulfur. As mentioned above, elemental sulfur is probably present in fluids upon sampling, which would therefore be available to react with sulfide and contribute to the discrepancy observed in Fig. 3. Because the oxidation state of polysulfide varies as a function of chain length, its presence could explain both the high redox balance ratios and inter-sample variability observed in Fig. 3. In addition to this completely abiotic mechanism, this process may be partly biologically-mediated. Polysulfide has been shown to be produced during sulfur oxidation by *Beggiatoa sp.* (Berg et al., 2014) and has been implicated in the reaction mechanism of sulfide:quinone oxidoreductase (Griesbeck et al., 2002), which is thought to be used by some *Epsilonproteobacteria* to oxidize sulfide (Yamamoto and Takai, 2011). In this biologically-mediated process, elemental sulfur produced by microbes during oxidation of sulfide presumably reacts with surrounding sulfide molecules, thereby consuming more sulfide without requiring any extra respiratory electron acceptor to be present.

As discussed above, oxygen is likely the preferred electron acceptor for microbial communities at *Crab Spa*. As a result, oxygen is highly depleted *in situ* (Table 2), and nitrate may serve as an important alternative electron acceptor. This role for nitrate as a secondary electron acceptor is consistent with its consumption during several incubations to which no oxygen was added (Figs. 2c, e, f). Because the method used in this study to quantify nitrate consumption actually measures the sum of nitrate + nitrite, the observed nitrate depletions (Fig. 2) indicate that nitrate was reduced beyond nitrite to either nitric oxide, nitrous oxide, nitrogen, or ammonium. Since the concentration of ammonium was also determined, our data provide a direct means to assess the relative importance of denitrification *vs* dissimilatory reduction to ammonium (DNRA), the two major nitrate removal processes

expected in this system. Ammonium, which is already present at elevated levels in *Crab Spa* fluids (11.5 μM, Table 2), increased in some incubations when either nitrate or hydrogen was added alone and in one control, suggesting slow rates of DNRA in these cases (Table 5, Fig. 2a, b, c). However, the amount of nitrate converted to ammonium was $\leq$9.4 μM and highly variable, representing 0–63% of the initial nitrate (Table 5).

In contrast, when both nitrate and hydrogen were added to the incubations (Figures 2e, 2f), the total amount of ammonium produced was not only consistent between replicates, but also of a much greater magnitude than with either amendment alone. While ammonium was produced in both incubations at 24°C and 50°C, the increase in cell counts was more consistent and ammonium production more pronounced at 50°C, supporting previous assertions that DNRA is a more important respiratory pathway at higher temperatures (Sievert and Vetriani, 2012). Despite the more rapid and greater extent of ammonium production at 50°C, the maximum amount of respired nitrate converted to ammonium was never greater than 55% (Table 5). Although we did observe evidence for ammonium assimilation during aerobic growth (Fig. 2d), similar levels of assimilation are unlikely to have accounted for more than 15 μM of the ~ 45-65 μM discrepancy. This suggests that denitrification to N_2 or other N intermediates was still occurring at a significant level at elevated temperatures. Indeed, denitrification has been reported for the moderate thermophilic epsilonproteobacterium *Nitratiruptor tergarcus* (Nakagawa et al., 2005; temperature optimum = 55°C).

Another important factor that likely constrained the proportion of nitrate converted to ammonium in our incubations is the type of electron donor. DNRA is typically supported by the oxidation of hydrogen, whereas denitrification can occur with either hydrogen or reduced sulfur (Sievert and Vetriani, 2012 and references therein). Since we observed both sulfide oxidation and hydrogen oxidation in the 50 °C incubation, it may be that the ammonium produced was directly coupled to hydrogen oxidation, whereas the sulfide consumption was coupled to denitrification. Indeed, the proportion of nitrate converted to ammonium closely mirrors the hydrogen consumed on an electron-equivalent level, while the remainder of nitrate loss not coupled to ammonium production can be sufficiently accounted for by sulfide consumption. Overall, these data suggest that the elevated ammonium concentrations observed in *Crab Spa* vent fluids may be the product of bacteria carrying out DNRA in the subseafloor and that hydrogen availability is an important factor determining whether or not ammonium is produced as a product of nitrate respiration in natural fluids.

4.3. Rates of chemosynthetic processes at in situ pressure and temperature

Rate measurements provide an important constraint on biological processes at vents. Previous studies incubating vent fluids at both *in situ* temperature and pressure are, to our knowledge, limited to an experiment conducted by Wirsen et al. (1986). Therefore, this study greatly expands the range of data and can be used for comparison of rates to recent studies that were not carried out at *in situ* pressure (Bourbonnais et al., 2012; Perner et al., 2010, 2011, 2013).

In our study, rates were derived for sulfide consumption/production, hydrogen consumption, nitrate consumption, oxygen consumption and ammonia production where at least two time points showed a consistent and measurable change in chemical concentrations. These data are presented as both cell-specific rates (Table 5) and as absolute rates (Supplemental spreadsheet). In general, per-cell sulfide consumption rates were consistent across all measured conditions, whereas nitrate consumption rates were more variable and greatly enhanced by the presence of dissolved hydrogen, particularly at 50 °C. Hydrogen oxidation rates were similarly variable, with the lowest values found where no electron acceptor was added (hydrogen-only amendment) and the highest rates found where nitrate was also added, with incubations at 50 °C further enhancing rates. Higher rates of ammonium production were correlated with faster rates of hydrogen oxidation, while sulfide production was only seen in the hydrogen-only treatment. Since oxygen was only measured in four cases, it is difficult to make specific conclusions regarding the rate of its consumption. Below, we discuss how these rates compare to other studies conducted on diffuse-flow vent fluids.

Similar to the present study, Perner et al. (2013) performed amendments of deep-sea vent fluids collected at various sites on the Mid-Atlantic Ridge and compared results to unamended samples. There are significant differences in rates between their study and ours, especially for absolute sulfide oxidation rates which were approximately half of those reported here. However, normalization of rates to total cell numbers yielded rates that are comparable. For example, sulfide consumption rates of 239–797 fmol H_2S cell^{-1} day^{-1} in the present study (Table 5) are consistent with the range of 1.7–432 fmol H_2S cell^{-1} day^{-1} reported by Perner et al. (2013) for sulfide addition experiments. Cell count normalized hydrogen oxidation rates in the range of 0.5–2208 fmol H_2 cell^{-1} day^{-1} determined by Perner et al. (2013) are similar to values of 49.6–1535 fmol H_2 cell^{-1} day^{-1} determined during this study (Table 5), although their slowest rates were approximately 2 orders of magnitude lower than ours. The reason for this discrepancy is difficult to ascertain, but Perner et al. (2011) note large changes in community composition relative to natural communities, which is an indicator that physicochemical conditions during their incubations changed appreciably from those found *in situ*. Such a change could indicate that not all microbes quantified in their incubations were active, possibly explaining lower per-cell rates. In contrast, our study saw only small changes in community composition, with the already-dominant *Epsilonproteobacteria* becoming more abundant as a result of incubations (Table 3).

Rates of nitrate consumption have also been determined in a variety of low temperature vent fluids from the Juan de Fuca Ridge by Bourbonnais et al. (2012) using isotope-labeled nitrogen additions to trace nitrate removal processes. In their study, denitrification rates ranged from $\sim 0.002-77$ fmol NO_3^- cell^{-1} day^{-1} (Easter Island and Hermosa vents, respectively) which represents a much larger range than in our study (58–655 fmol NO_3^- cell^{-1} day^{-1}, Table 5). While their highest denitrification rates compare well with our nitrate-only additions, a number of their incubations reported orders of magnitude lower denitrification rates compared to our study. It is unclear why there is such a large difference, since the cell densities in the source fluids used by Bourbonnais et al. (2012) are in the same range as the present study and were also mostly dominated by *Epsilonproteobacteria*. One key difference between studies is the concentration of nitrate amendments; in the present study, we used concentrations approximately ten-fold higher. Since Bourbonnais et al. (2012) show that natural nitrate deficits were negatively correlated with denitrification rates, this could imply that samples with large nitrate deficits may have had lower abundances of denitrifiers or that cells present were not expressing denitrification enzymes. Since our study site has similar nitrate deficits (Table 2), yet we observed high per-cell denitrification rates (Table 5), it could be that higher concentrations of amendments permitted the reactivation of these pathways or the growth of denitrifiers. It is also possible that either decompression or experimental manipulation of fluids (or a combination of these factors) accounts for the large range of values observed in their study. Bourbonnais et al. (2012) report that

fluids were purged with helium in some cases prior to incubation, and were allowed to remain at room temperature for 12 h prior to measurements in other cases - both of which could affect rate measurements. Purging removes volatile redox-active species such as sulfide, hydrogen, and methane, and since our results show that holding samples for 12 h in sealed vessels will deplete all available electron acceptors, not just oxygen (Fig. 2a, b), microbes in either of these situations would have been deprived of energy sources for growth. As a result, they may have died or become less active, possibly accounting for some of the lower rates. Moreover, if most autotrophic energy sources were removed due to purging or consumption, the rates reported by these authors may represent background levels of heterotrophic denitrification instead of autotrophic processes.

Bourbonnais et al. (2012) also showed that denitrification was the dominant nitrate removal process, with rates exceeding those of DNRA by up to 160-fold. In the presence of hydrogen, the present study demonstrates significantly higher rates of DNRA and that the proportion of NO_3^- respired *via* DNRA was only 3-9-fold lower than denitrification. Since dissolved hydrogen is thought to be the main electron donor for DNRA (discussion above; Sievert and Vetriani, 2012 and references therein), experimental approaches that provide hydrogen as an amendment may represent a more accurate constraint on potential DNRA rates in the natural environment.

Total nitrogen loss in the subseafloor biosphere was also calculated by Bourbonnais et al. (2012) by multiplying denitrification rates determined in their study with fluid flux and estimated residence time of the fluids. If the rates of denitrification determined in our study are used as input for this calculation, it would make nitrate removal processes by the global deep-sea vent subseafloor microbial community a much more significant sink in the global N-cycle, bringing it into the range of benthic denitrification (Bourbonnais et al., 2012; Gruber, 2004; Codispoti, 2007). While this suggests that denitrification at vents may have been underestimated, there are several important caveats. As discussed above, oxygen was more rapidly consumed than nitrate in our incubations, and yielded a higher number of cells (Fig. 2). Therefore, it is likely that in natural environments oxygen is the preferred electron acceptor, and that denitrification will be suppressed where oxygen is non-limiting, although there may be a threshold below which so-called "aerobic denitrification" occurs (Fig. 2d and Supplemental spreadsheet; Gao et al., 2009). In addition, the residence time of fluids within a subsurface biosphere and the mixing ratio between seawater and vent fluid should ultimately control oxygen concentrations in low temperature hydrothermal vent fluids, and therefore denitrification rates. Higher proportions of seawater will introduce more oxygen and shorter residence times will reduce the opportunity for resident microbes to completely consume oxygen present. Although the mixing ratio can be well-constrained based on fluid composition, residence time and the extent of "aerobic denitrification" are relatively unknown, demonstrating a need for more research to accurately constrain nitrogen loss in the subseafloor biosphere.

5. Summary

In the present study, novel methods were developed that allowed IGT samplers to be used for incubations of deep-sea hydrothermal vent microbial communities under simulated seafloor conditions. IGT samplers were modified to allow both initial amendments and subsamples during short, ~24 h incubations, permitting time-series measurements of chemical concentrations. Results from eighteen incubations, representing seven separate treatments in biological replicates, provide the basis for future biogeochemical models and reveal important gaps in our understanding of microbially-catalyzed processes at deep-sea hydrothermal vents. Data generated in this study have confirmed predicted microbial processes, quantified their rates, and revealed insights into the stoichiometry of metabolically relevant redox reactions. In addition, because incubations were short ($\leq$1 day) and amendment concentrations low (~100 μM), the microbial community composition was minimally altered from background communities. Therefore, the results reported here may be representative of rates in the natural environment and can be further combined with vent fluid chemistry to constrain hydrothermal vent microbial communities' contributions to biogeochemical cycling. Finally, since these methods can be applied to any pelagic deep-sea microbial community, incubations conducted in IGT samplers have great potential to increase our understanding of microbial processes and their quantitative importance in a broad range of deep-sea environments.

Acknowledgements

We thank the officers, crew, and pilots of the R/V *Atlantis* and ROV *Jason* for their expert help at sea and their outstanding efforts acquiring the samples needed for this study. We also thank the scientific party for support, with special thanks going to Kerry McCulloch, Miriam Sollich, and Xi Wei for invaluable help with shipboard lab experiments. Many thanks are also due to Ben van Mooy for lending his lab's oxygen optode system, to Scott Wankel, Carly Buchwald and Zoe Sandwith for help quantifying nitrate/nitrite after the cruise, to Niculina Musat for assistance with CARD-FISH, to Virginia Edgcomb for lending her lab's Aanderaa *in situ* oxygen optode, and to Jeremy Rich for providing nitrate measurements for background seawater.

This research was funded by a grant of the Dimensions of Biodiversity program of the National Science Foundation to S.M.S, J.S.S., and C.D.T (NSF-OCE-1136727). Funding for J.M. was provided by doctoral fellowships from the National Sciences and Engineering Research Council of Canada (NSERC-PGSD3) and the National Aeronautics and Space Administration Earth Systems Science Fellowship (NESSF), an award from the Canadian Meteorological and Oceanographic Society, as well as funding from WHOI academic programs and the aforementioned National Science Foundation grant.

Appendix A. Supplemental material

Supplemental data associated with this article can be found in the online version at http://dx.doi.org/10.1016/j.dsr.2016.06.011.

References

Amend, J.P., McCollom, T.M., Hentscher, M., Bach, W., 2011. Catabolic and anabolic energy for chemolithoautotrophs in deep-sea hydrothermal systems hosted in different rock types. Geochim. Cosmochim. Acta 75, 5736–5748.

Bartlett, D.H., 2002. Pressure effects on in vivo microbial processes. Biochim. Biophys. Acta BBA - Protein Struct. Mol. Enzymol. 1595, 367–381.

Berg, J.S., Schwedt, A., Kreutzmann, A.-C., Kuypers, M.M.M., Milucka, J., 2014. Polysulfides as intermediates in the oxidation of sulfide to sulfate by *Beggiatoa* spp. Appl. Environ. Microbiol. 80 (2), 629–636.

Bianchi, A., Garcin, J., Tholosan, O., 1999. A high-pressure serial sampler to measure microbial activity in the deep sea. Deep Sea Res. Part Oceanogr. Res. Pap. 46, 2129–2142.

Bourbonnais, A., Juniper, S.K., Butterfield, D.A., Devol, A.H., Kuypers, M.M.M., Lavik, G., Hallam, S.J., Wenk, C.B., Chang, B.X., Murdock, S.A., Lehmann, M.F., 2012. Activity and abundance of denitrifying bacteria in the subsurface biosphere of diffuse hydrothermal vents of the Juan de Fuca Ridge. Biogeosciences 9, 4661–4678.

Butterfield, D.A., Roe, K.K., Lilley, M.D., Huber, J.A., Baross, J.A., Embley, R.W., Massoth, G.J., 2004. Mixing, reaction and microbial activity in the sub-seafloor revealed by temporal and spatial variation in diffuse flow vents at axial volcano. In: Wilcock, W.S.D., Delong, E.F., Kelley, D.S., Baross, J.A., Cary, S.C. (Eds.), The Subseafloor Biosphere at Mid-Ocean Ridges. American Geophysical Union, Washington DC, USA, pp. 269–289.

Charlou, J.L., Donval, J.P., Douville, E., Jean-Baptiste, P., Radford-Knoery, J., Fouquet, Y., Dapoigny, A., Stievenard, M., 2000. Compared geochemical signatures and the evolution of Menez Gwen (37°50′N) and Lucky Strike (37°17′N) hydrothermal fluids, south of the Azores Triple Junction on the Mid-Atlantic Ridge. Chem. Geol. 171, 49–75.

Chen, J., Strous, M., 2013. Denitrification and aerobic respiration, hybrid electron transport chains and co-evolution. Biochim. Biophys. Acta BBA - Bioenerg. 1827, 136–144.

Codispoti, L.A., 2007. An oceanic fixed nitrogen sink exceeding 400 Tg N a^{-1} vs the concept of homeostasis in the fixed-nitrogen inventory. Biogeosciences 4, 233–253.

Dahle, H., Økland, I., Thorseth, I.H., Pederesen, R.B., Steen, I.H., 2015. Energy landscapes shape microbial communities in hydrothermal systems on the Arctic Mid-Ocean Ridge. ISME J. 9, 1593–1606.

Daims, H., Brühl, A., Amann, R., Schleifer, K.-H., Wagner, M., 1999. The domain-specific probe EUB338 is insufficient for the detection of all bacteria: development and evaluation of a more comprehensive probe set. Syst. Appl. Microbiol. 22, 434–444.

Flores, G.E., Campbell, J.H., Kirshtein, J.D., Meneghin, J., Podar, M., Steinberg, J.I., Seewald, J.S., Tivey, M.K., Voytek, M.A., Yang, Z.K., Reysenbach, A.-L., 2011. Microbial community structure of hydrothermal deposits from geochemically different vent fields along the Mid-Atlantic Ridge: microbial communities of hydrothermal vent deposits. Environ. Microbiol. 13 (8), 2158–2171.

Flores, G.E., Wagner, I.D., Liu, Y., Reysenbach, A.-L., 2012. Distribution, Abundance, and Diversity Patterns of the Thermoacidophilic "Deep-Sea Hydrothermal Vent Euryarchaeota 2". Front. Microbiol. 3, 47.

Foustoukos, D.I., Houghton, J.L., Seyfried Jr., W.E., Sievert, S.M., Cody, G.D., 2011. Kinetics of H_2–O_2–H_2O redox equilibria and formation of metastable H_2O_2 under low temperature hydrothermal conditions. Geochim. Cosmochim. Acta 75, 1594–1607.

Gao, H., Schreiber, F., Collins, G., Jensen, M.M., Kostka, J.E., Lavik, G., de Beer, D., Zhou, H., Kuypers, M.M.M., 2009. Aerobic denitrification in permeable Wadden Sea sediments. ISME J. 4, 417–426.

Garside, C., 1982. A chemiluminescent technique for the determination of nanomolar concentrations of nitrate and nitrite in seawater. Mar. Chem. 11 (2), 159–167.

Greuter, D., Loy, A., Horn, M., Rattei, T., 2016. probeBase—an online resource for rRNA-targeted oligonucleotide probes and primers: new features 2016. Nucl. Acids Res. 44, D586–D589.

Griesbeck, C., Schütz, M., Schödl, T., Bathe, S., Nausch, L., Mederer, N., Vielreicher, M., Hauska, G., 2002. Mechanism of sulfide-quinone reductase investigated using site-directed mutagenesis and sulfur analysis. Biochemistry 41, 11552–11565.

Gruber, N., 2004. The dynamics of the marine nitrogen cycle and its influence on atmospheric CO_2 variations. In: Follows, M., Oguz, T. (Eds.), The Ocean Carbon Cycle and Climate, NATO Science Series. Springer, The Netherlands, pp. 97–148.

Hall, P., Aller, R., 1992. Rapid, small-volume, flow injection analysis for ΣCO_2 and NH_4^+ in marine and fresh-waters. Limnol. Oceanogr. 37 (5), 1113–1119.

Han, Y., Perner, M., 2014. The role of hydrogen for *Sulfurimonas denitrificans*'. Metab. PLoS ONE 9 (8), e106218.

Hedderich, R., Klimmek, O., Kröger, A., Dirmeier, R., Keller, M., Stetter, K.O., 1998. Anaerobic respiration with elemental sulfur and with disulfides. FEMS Microbiol. Rev. 22, 353–381.

Hentscher, M., Bach, W., 2012. Geochemically induced shifts in catabolic energy yields explain past ecological changes of diffuse vents in the East Pacific Rise 9° 50′N area. Geochem. Trans. 13, 1.

Huber, J.A., Mark Welch, D.B., Morrison, H.G., Huse, S.M., Neal, P.R., Butterfield, D.A., Sogin, M.L., 2007. Microbial population structures in the deep marine biosphere. Science 318, 97–100.

Jannasch, H.W., Mottl, M.J., 1985. Geomicrobiology of deep-sea hydrothermal vents. Science 229, 717.

Lin, X., Wakeham, S.G., Putnam, I.F., Astor, Y.M., Scranton, M.I., Chistoserdov, A.Y., Taylor, G.T., 2006. Comparison of vertical distributions of prokaryotic assemblages in the anoxic cariaco basin and black sea by use of fluorescence in situ hybridization. Appl. Environ. Microbiol. 72, 2679–2690.

Luther, G.W., Findlay, A.J., MacDonald, D.J., Owings, S.M., Hanson, T.E., Beinart, R.A., Girguis, P.R., 2011. Thermodynamics and kinetics of sulfide oxidation by oxygen: a look at inorganically controlled reactions and biologically mediated processes in the environment. Front. Microbiol. 2, 62.

Meier, D.V., Bach, W., Girguis, P.R., Gruber-Vodicka, H.R., Reeves, E.P., Richter, M., Vidoudez, C., Amann, R., Meyerdierks, A., 2016. Heterotrophic *Proteobacteria* in the vicinity of diffuse hydrothermal venting. Environ. Microbiol. . http://dx.doi.org/10.1111/1462-2920.13304

Mino, S., Kudo, H., Takayuki, A., Sawabe, T., Takai, K., Nakagawa, S., 2014. *Sulfurovum aggregans* sp. nov., a novel hydrogen-oxidizing, thiosulfate-reducing chemolithoautotroph within the *Epsilonproteobacteria* isolated from a deep-sea hydrothermal vent chimney at the Central Indian Ridge, and an emended description of the genus *Sulfurovum*. Int. J. Syst. Evol. Microbiol. 64, 3195–3201.

Nakagawa, S., Takai, K., Inagaki, F., Horikoshi, K., Sako, Y., 2005. *Nitratiruptor tergarcus* gen. nov., sp. nov. and *Nitratifractor salsuginis* gen. nov., sp. nov., nitrate-reducing chemolithoautotrophs of the ε-Proteobacteria isolated from a deep-sea hydrothermal system in the Mid-Okinawa Trough. Int. J. Syst. Evol. Microbiol. 55, 925–933.

Nakagawa, S., Takai, K., 2008. Deep-sea vent chemoautotrophs: diversity, biochemistry and ecological significance. FEMS Microbiol. Ecol. 65 (1), 1–14.

Perner, M., Petersen, J.M., Zielinski, F., Gennerich, H.-H., Seifert, R., 2010. Geochemical constraints on the diversity and activity of H_2-oxidizing microorganisms in diffuse hydrothermal fluids from a basalt- and an ultramafic-hosted vent. FEMS Microbiol. Ecol. 74, 55–71.

Perner, M., Hentscher, M., Rychlik, N., Seifert, R., Strauss, H., Bach, W., 2011. Driving forces behind the biotope structures in two low-temperature hydrothermal venting sites on the southern Mid-Atlantic Ridge. Environ. Microbiol. Rep. 3, 727–737.

Perner, M., Hansen, M., Seifert, R., Strauss, H., Koschinsky, A., Petersen, S., 2013. Linking geology, fluid chemistry, and microbial activity of basalt- and ultramafic-hosted deep-sea hydrothermal vent environments. Geobiology 11, 340–355.

Proskurowski, G., Lilley, M.D., Olson, E.J., 2008. Stable isotopic evidence in support of active microbial methane cycling in low-temperature diffuse flow vents at 9°50′N East Pacific Rise. Geochim. Cosmochim. Acta 72, 2005–2023.

Reeves, E.P., McDermott, J.M., Seewald, J.S., 2014. The origin of methanethiol in midocean ridge hydrothermal fluids. Proc. Natl. Acad. Sci. 111, 5474–5479.

Seewald, J.S., Doherty, K.W., Hammar, T.R., Liberatore, S.P., 2002. A new gas-tight isobaric sampler for hydrothermal fluids. Deep Sea Res. Part I: Oceanogr. Res. Pap. 49, 189–196.

Sievert, S.M., Vetriani, C., 2012. Chemoautotrophy at deep-sea vents: past, present. Future Oceanogr. 25 (1), 218–233.

Sievert, S.M., Wieringa, E.B.A., Wirsen, C.O., Taylor, C.D., 2007. Growth and mechanism of filamentous-sulfur formation by *Candidatus* Arcobacter sulfidicus in opposing oxygen-sulfide gradients. Environ. Microbiol. 9 (1), 271–276.

Takai, K., Suzuki, M., Nakagawa, S., Miyazaki, M., Suzuki, Y., Inagaki, F., Horikoshi, K., 2006. *Sulfurimonas paralvinellae* Sp. Nov., a novel mesophilic, hydrogen- and sulfur-oxidizing chemolithoautotroph within the *Epsilonproteobacteria* isolated from a deep-sea hydrothermal vent polychaete nest, reclassification of *Thiomicrospira denitrificans* as *Sulfurimonas denitrificans* Comb. Nov. and emended description of the genus *Sulfurimonas*. Int. J. Syst. Evol. Microbiol. 56, 1725–1733.

Timmer-Ten Hoor, A., 1981. Cell yield and bioenergetics of *Thiomicrospira denitrificans* compared with *Thiobacillus denitrificans*. Antonie Van Leeuwenhoek 47, 231–243.

Von Damm, K.L., Lilley, M.D., 2004. Diffuse Flow Hydrothermal Fluids from 9° 50′ N East Pacific Rise: Origin, (Evolution and Biogeochemical) Controls, in. In: Wilcock, W.S.D., Delong, E.F., Kelley, D.S., Baross, J.A., Cary, S.C. (Eds.), the Subseafloor Biosphere at Mid-ocean Ridges. American Geophysical Union, pp. 245–268.

Wankel, S.D., Germanovich, L.N., Lilley, M.D., Genc, G., DiPerna, C.J., Bradley, A.S., Olson, E.J., Girguis, P.R., 2011. Influence of subsurface biosphere on geochemical fluxes from diffuse hydrothermal fluids. Nat. Geosci. 4, 461–468.

Wirsen, C.O., Tuttle, J.H., Jannasch, H.W., 1986. Activities of sulfur-oxidizing bacteria at the 21 N East Pacific Rise vent site. Mar. Biol. 92, 449–456.

Wirsen, C.O., Sievert, S.M., Cavanaugh, C.M., Molyneaux, S.J., Ahmad, A., Taylor, L.T., DeLong, E.F., Taylor, C.D., 2002. Characterization of an autotrophic sulfide-oxidizing marine *Arcobacter* sp. That produces filamentous sulfur. Appl. Environ. Microbiol. 68 (1), 316–325.

Yamamoto, M., Takai, K., 2011. Sulfur metabolisms in epsilon- and gamma-proteobacteria in deep-sea hydrothermal fields. Front. Microbiol. 2, 192.